

CMOS-compatible Si-wire polarization beam splitter based on wavelength-insensitive coupler

Yusuke Sawada^{a)}, Takeshi Fujisawa, Takanori Sato,
and Kunimasa Saitoh

*Graduate School of Information Science and Technology, Hokkaido University,
North 14, West 9, Kita-ku, Sapporo 060–0814, Japan*

a) sawada@icp.ist.hokudai.ac.jp

Abstract: An ultrabroadband silicon polarization beam splitter (PBS) based on a wavelength-insensitive coupler is fabricated by a standard complementary metal oxide semiconductor technology. The PBS has three identical directional couplers and two identical delay lines with a point symmetric layout. We experimentally demonstrate the broadband operation of the PBS. The crosstalk is less than –12 dB for both TE and TM modes over the wavelength range from 1532 nm to 1649 nm. Additionally, we theoretically discuss a tunability of the PBS for the first time.

Keywords: silicon photonics, waveguide devices, polarization beam splitter

Classification: Integrated optoelectronics

References

- [1] T. Barwicz, *et al.*: “Polarization-transparent microphotonic devices in the strong confinement limit,” *Nat. Photonics* **1** (2007) 57 (DOI: [10.1038/nphoton.2006.41](https://doi.org/10.1038/nphoton.2006.41)).
- [2] H. Fukuda, *et al.*: “Silicon photonic circuit with polarization diversity,” *Opt. Express* **16** (2008) 4872 (DOI: [10.1364/OE.16.004872](https://doi.org/10.1364/OE.16.004872)).
- [3] H. Fukuda, *et al.*: “Ultrasmall polarization splitter based on silicon wire waveguides,” *Opt. Express* **14** (2006) 12401 (DOI: [10.1364/OE.14.012401](https://doi.org/10.1364/OE.14.012401)).
- [4] D. Dai, *et al.*: “Ultrashort broadband polarization beam splitter based on an asymmetrical directional coupler,” *Opt. Lett.* **36** (2011) 2590 (DOI: [10.1364/OL.36.002590](https://doi.org/10.1364/OL.36.002590)).
- [5] D. Dai, *et al.*: “Novel ultra-short and ultra-broadband polarization beam splitter based on a bent directional coupler,” *Opt. Express* **19** (2011) 18614 (DOI: [10.1364/OE.19.018614](https://doi.org/10.1364/OE.19.018614)).
- [6] D. Dai, *et al.*: “Silicon polarization beam splitter based on an asymmetrical evanescent coupling system with three optical waveguides,” *J. Lightwave Technol.* **30** (2012) 3281 (DOI: [10.1109/JLT.2012.2218217](https://doi.org/10.1109/JLT.2012.2218217)).
- [7] J. Wang, *et al.*: “Realization of an ultra-short silicon polarization beam splitter with an asymmetrical bent directional coupler,” *Opt. Lett.* **38** (2013) 4 (DOI: [10.1364/OL.38.000004](https://doi.org/10.1364/OL.38.000004)).
- [8] T. Uematsu, *et al.*: “Ultra-broadband silicon-wire polarization beam combiner/splitter based on a wavelength insensitive coupler with a point-symmetrical configuration,” *IEEE Photon. J.* **6** (2014) 4500108 (DOI: [10.1109/JPHOT.2014.2355555](https://doi.org/10.1109/JPHOT.2014.2355555)).

- 2014.2302808).
- [9] Z. Lu, *et al.*: “Wideband silicon photonic polarization beamsplitter based on point-symmetric cascaded broadband couplers,” *Opt. Express* **23** (2015) 29413 (DOI: [10.1364/OE.23.029413](https://doi.org/10.1364/OE.23.029413)).
 - [10] B. Yang, *et al.*: “Ultrashort polarization splitter using two-mode interference in silicon photonic wires,” *IEEE Photonics Technol. Lett.* **21** (2009) 432 (DOI: [10.1109/LPT.2009.2013638](https://doi.org/10.1109/LPT.2009.2013638)).
 - [11] A. Hosseini, *et al.*: “Ultracompact and fabrication-tolerant integrated polarization splitter,” *Opt. Lett.* **36** (2011) 4047 (DOI: [10.1364/OL.36.004047](https://doi.org/10.1364/OL.36.004047)).
 - [12] Y. Zhang, *et al.*: “High-extinction-ratio silicon polarization beam splitter with tolerance to waveguide width and coupling length variations,” *Opt. Express* **24** (2016) 6586 (DOI: [10.1364/OE.24.006586](https://doi.org/10.1364/OE.24.006586)).
 - [13] K. Jinguji, *et al.*: “Two-port optical wavelength circuits composed of cascaded Mach-Zehnder interferometers with point-symmetrical configurations,” *J. Lightwave Technol.* **14** (1996) 2301 (DOI: [10.1109/50.541222](https://doi.org/10.1109/50.541222)).
 - [14] Y. Ishizaka, *et al.*: “Three-dimensional finite-element solutions for crossing slot-waveguides with finite core-height,” *J. Lightwave Technol.* **30** (2012) 3394 (DOI: [10.1109/JLT.2012.2217478](https://doi.org/10.1109/JLT.2012.2217478)).
 - [15] T. Fujisawa, *et al.*: “Low-loss, compact, and fabrication-tolerant Si-wire 90° waveguide bend using clothoid and normal curves for large scale photonic integrated circuits,” *Opt. Express* **25** (2017) 9150 (DOI: [10.1364/OE.25.009150](https://doi.org/10.1364/OE.25.009150)).
 - [16] Y. Sawada, *et al.*: “Development of the wavefront matching method based on the 3-D finite-element method and its application to Si-wire mode converters,” *J. Lightwave Technol.* **36** (2018) 3652 (DOI: [10.1109/JLT.2018.2843383](https://doi.org/10.1109/JLT.2018.2843383)).
 - [17] M. Shinkawa, *et al.*: “Nonlinear enhancement in photonic crystal slow light waveguides fabricated using CMOS-compatible process,” *Opt. Express* **19** (2011) 22208 (DOI: [10.1364/OE.19.022208](https://doi.org/10.1364/OE.19.022208)).

1 Introduction

Silicon photonics has attracted much attention because it provides high-density integration and is suitable for mass production using a standard complementary metal oxide semiconductor (CMOS) technology. High-index contrast of silicon-based waveguide devices greatly contributes to reduction in footprint, whereas they introduce the large polarization dependence. In optical fiber transmission systems, since the state of the polarization is randomly changed in standard single mode fiber (SMF), and therefore, so-called polarization diversity scheme [1, 2] is employed in the receiver and a polarization beam splitter (PBS) and a polarization rotator are necessary.

Recently, various types of silicon-based PBSs have been proposed based on directional couplers (DCs) [3, 4, 5, 6, 7, 8, 9], multimode interference couplers [10, 11], gratings [12], and Mach-Zehnder interferometers [13]. Among them, DCs are simple structure and easy to design. So, many ideas, such as asymmetric DCs [4, 6] and bent DCs [5, 7], are realized for high-performance polarization splitting. Generally, DCs have large wavelength dependence and parabolic transmission spectra, which is typical for DCs, are unavoidable. Therefore, it is difficult to obtain the broadband operation of DC-based PBSs. In [8, 9], PBSs based on two-cascaded 3-dB DCs were proposed to overcome the problem. In our previous

paper [8], a PBS based on a wavelength-insensitive coupler (WINC) composed of rounded delay lines with a point symmetric layout [13] was theoretically proposed. In this paper, we experimentally demonstrate the broadband operation of the WINC-based PBS. A simple photolithography is used for the patterning waveguide structure in the fabrication process of the PBS, while an electron-beam lithography is used for most previous reports [3, 7, 9, 10, 12, 11]. Also, the tunability of the PBS is theoretically discussed for the first time.

2 Fabrication and operation principle of WINC-based PBS

Fig. 1(a) shows the schematic of the WINC-based PBS. It consists of three identical DCs and two sets of delay line waveguides. The waveguides are Si-wire waveguides and the cladding material is silica. We redesigned the PBS based on three-dimensional finite-element method (FEM) [14, 15, 16] since the cladding material of PBS in our earlier report [8] was air. The waveguide widths w_1 and w_2 are both 500 nm, the waveguide gap is 400 nm, the coupling lengths L_0 and L_1 are 9.63 μm and 8.388 μm , respectively, and the angle and radius of delay lines are determined so that the phase shift is around $\pi/3$ ($\theta = \pi/11.77$ and $R = 21 \mu\text{m}$). TM mode launched from Port 1 is equally separated (3 dB operation) at the center of the second DC. After that, separated TM mode propagates the counterpart waveguide of the point symmetric structure, and then TM mode is output to Port 4 because of the optical reciprocity. On the other hand, TE mode launched from Port 1 hardly couples in three identical DCs because the coupling lengths of three identical couplers are too short for TE mode, and then TE mode is output to Port 3.

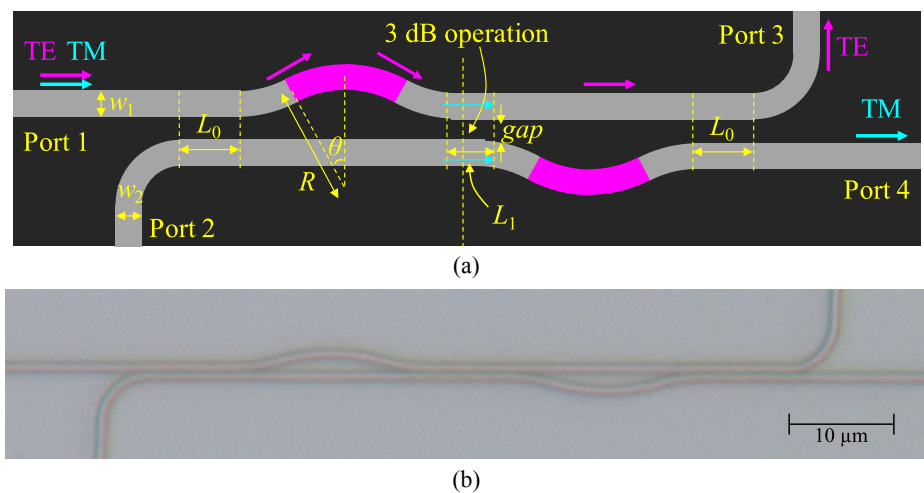


Fig. 1. (a) The schematic of the WINC-based PBS and (b) the microscope picture of the fabricated PBS.

The redesigned WINC-based PBS, which has a point symmetric structure, is fabricated by a standard CMOS technology, in which a photolithography (KrF, 248 nm) was used for the patterning waveguide structure. The inverse taper spot size converter [17] is used to launch light into the chip. Fig. 1(b) shows the microscope picture of the fabricated PBS.

3 Results and discussion

A tunable laser (1500 to 1650 nm) is used for the light source and TE- or TM-fundamental mode is launched to the chip through the inverse taper spot size converter. The output light is measured by an optical spectrum analyzer (OSA). Figs. 2(a) and (b) show the measured and calculated transmission spectra of the WINC-based PBS when (a) TE and (b) TM mode is launched. The measurement is implemented 10 times continuously and their average is shown. The plotted measurement results are smoothed by a moving average method for visibility. For both modes, the transmission (Port 3 for TE and Port 4 for TM modes) is very flat over the broad wavelength range and agree well with the calculated results. For the crosstalk (Port 4 for TE and Port 3 for TM modes), the peak wavelength is shifted to longer wavelength side for the TM mode (1550 nm for the calculation and 1600 nm for the measurement). This is probably due to the fabrication error in the waveguided width. The insertion loss is lower than 1 dB for all measurable wavelength range in our experimental setup (1500 to 1650 nm). Fig. 3 shows the extinction ratio (ER) of the WINC-based PBS. The ER for TE and TM modes are defined as follows:

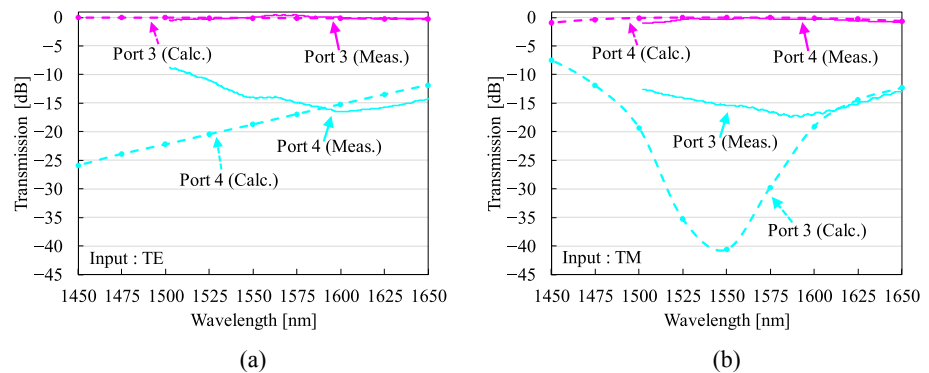


Fig. 2. The measured and calculated transmission spectra of the WINC-based PBS when (a) TE and (b) TM mode is launched.

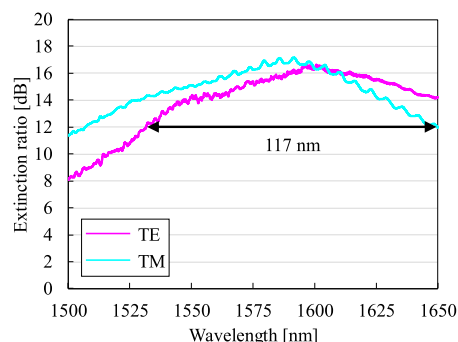


Fig. 3. The extinction ratio of the WINC-based PBS.

$$\begin{aligned} (\text{Extinction ratio for TE mode}) &= 10 \log_{10} \frac{P_{\text{TE,Port 3}}}{P_{\text{TE,Port 4}}} \\ (\text{Extinction ratio for TM mode}) &= 10 \log_{10} \frac{P_{\text{TM,Port 4}}}{P_{\text{TM,Port 3}}} \end{aligned} \quad (1)$$

$P_{\text{TE,Port 3}}$ and $P_{\text{TE,Port 4}}$ denote the transmission to Port 3 and Port 4 when TE mode is launched from Port 1. $P_{\text{TM,Port 3}}$ and $P_{\text{TM,Port 4}}$ denote the transmission to Port 3 and Port 4 when TM mode is launched from Port 1. The ER for TE and TM modes simultaneously achieve more than 12 dB over the wavelength range from 1532 nm to 1649 nm (117 nm). It can be inferred that the higher ER is obtained in case that the high-accuracy fabrication process, such as an electron-beam lithography, is used.

Additionally, we theoretically discuss the tunability of the PBS. Since the WINC-based PBS has two delay lines, the refractive-index of one of the delay line waveguides can be changed by, for example, a heater. Therefore, it is expected that a tunable WINC-based PBS can be realized. Here, the refractive-index of one of the delay line waveguides (magenta area in Fig. 1(a)) is changed by 0.01 and 0.02. The value can be reduced by changing the length of delay line waveguides while keeping the $\pi/3$ phase difference. Figs. 4(a) and (b) show the calculated transmission spectra for (a) TE and (b) TM mode when the refractive-index shifts are assumed. It can be seen that transmission spectra shift with the refractive-index changes. The results demonstrate the tunability of the WINC-based PBS when heaters are placed on delay lines. The tunability may be used for post-fab trimming or a novel functionality for controlling the polarization. In the previous PBS based on DCs [3, 4, 5, 6, 7], it is difficult to add tunability because two waveguides are too close to place the heater for one of the waveguides. With the same reason, it is also difficult to add the tunability for the waveguide-width-changed cascaded-DC-based PBS [9]. Therefore, adding the tunability is one of the advantages of the proposed PBS.

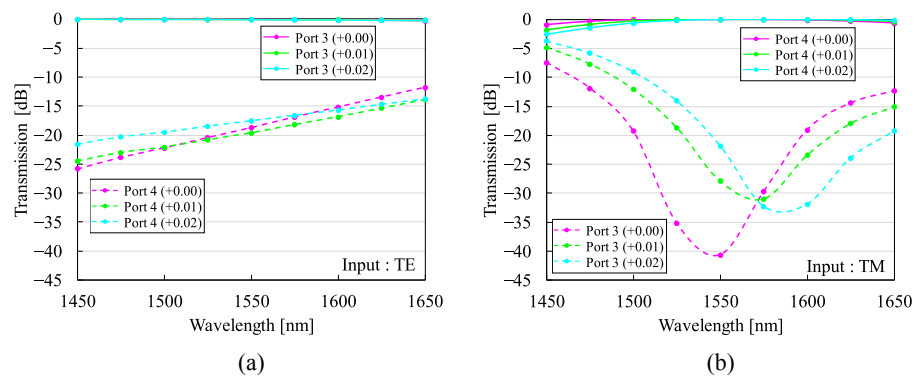


Fig. 4. The calculated transmission spectra for (a) TE and (b) TM mode when refractive-index shifts are assumed.

4 Conclusion

We have experimentally demonstrated the broadband operation and low insertion loss of the WINC-based PBS fabricated by a simple photolithography. The PBS

achieved 12-dB ER over the wavelength range of 117 nm for TE and TM modes simultaneously and 1-dB insertion loss in wide wavelength range. The tunability of the PBS is theoretically discussed for the first time and the proposed PBS can be tunable by adding the heater on one of the delay lines.